A Simple and Scalable Representation for Graph Generation

Yunhui Jang[1], **Seul Lee**[2], **Sungsoo Ahn**[1]
[1]Pohang University of Science and Technology [2]KAIST
`{uni5510,sungsoo.ahn}@postech.ac.kr, seul.lee@kaist.ac.kr`

Abstract

Recently, there has been a surge of interest in employing neural networks for graph generation, a fundamental statistical learning problem with critical applications like molecule design and community analysis. However, most approaches encounter significant limitations when generating large-scale graphs. This is due to their requirement to output the full adjacency matrices whose size grows quadratically with the number of nodes. In response to this challenge, we introduce a new, simple, and scalable graph representation named gap encoded edge list (GEEL) that has a small representation size that aligns with the number of edges. In addition, GEEL significantly reduces the vocabulary size by incorporating the gap encoding and bandwidth restriction schemes. GEEL can be autoregressively generated with the incorporation of node positional encoding, and we further extend GEEL to deal with attributed graphs by designing a new grammar. Our findings reveal that the adoption of this compact representation not only enhances scalability but also bolsters performance by simplifying the graph generation process. We conduct a comprehensive evaluation across ten non-attributed and two molecular graph generation tasks, demonstrating the effectiveness of GEEL.

1 Introduction

Learning the distribution over graphs is a challenging problem across various domains, including social network analysis [1] and molecular design [2, 3]. Recently, neural networks gained much attention in addressing this challenge by leveraging the advancements in deep generative models, e.g., diffusion models [4], to show promising results.

However, the majority of the graph generative models do not scale to large graphs, since they generate the adjacency matrix-based graph representations [5, 6, 7, 3]. In particular, for large graphs with N nodes, the adjacency matrix is hard to handle since they consist of N^2 binary elements. For example, employing a Transformer-based autoregressive model for all the binary elements requires $O(N^4)$ computational complexity. Researchers have considered tree-based [8] or motif-based representations [9, 10] to mitigate this issue, but these representations constrain the graphs being generated, e.g., molecules or graphs with motifs extracted from training data.

Intriguingly, a few works [11, 12] have considered generating the edge list representations as a potential solution for large-scale graph generation. In particular, the list contains M edges that are fewer than N^2 elements in the adjacency matrix, a distinctive difference especially for sparse graphs. However, such edge list-based graph generative models instead suffer from the vast vocabulary size N^2 for the possible edges. Consequently, they face the challenge of learning dependencies over a larger output space and may overfit to a specific edge or an edge combination appearing only in a few samples. Indeed, the edge list-based representations empirically perform even worse than simple adjacency matrix-based models [13], e.g., see Table 1.

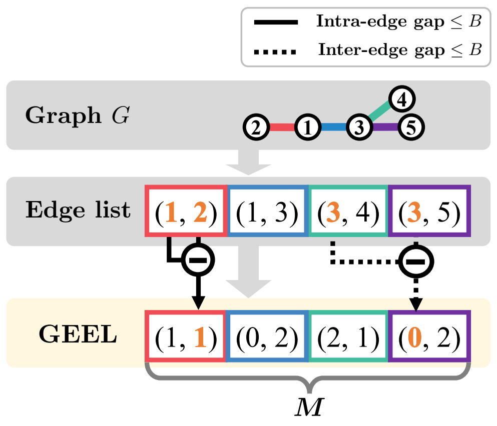

(a) Overview.

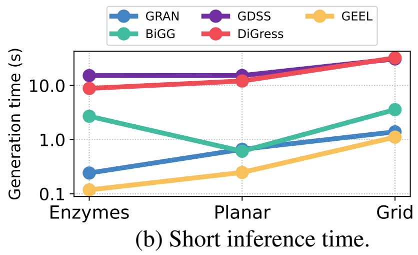

(b) Short inference time.

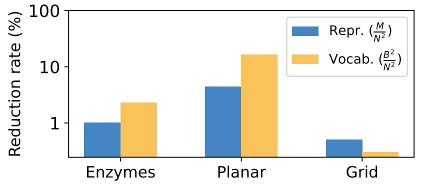

(c) Rep. and vocab. size reduction.

Figure 1: **Overview and advantages of gap encoded edge list (GEEL).**

In this paper, we propose a simple, scalable, yet effective graph representation for graph generation, coined **G**ap **E**ncoded **E**dge **L**ist (GEEL). On one hand, grounded in edge lists, GEEL enjoys a compact representation size that aligns with the number of edges. On the other hand, GEEL improves the edge list representations by significantly reducing the vocabulary size with gap encodings that replace the node indices with the difference between nodes, i.e., gap, as described in Figure 1a. We also promote bandwidth restriction [14] which further reduces the vocabulary size. Next, we augment the GEEL generation with node positional encoding. Finally, we introduce a new grammar for the extension of GEEL to attributed graphs.

The advantages of our GEEL are primarily twofold: scalability and efficacy. First, regarding scalability, the reduced representation and the vocabulary sizes mitigate the computational and memory complexity, especially for sparse graphs, as described in Figure 1b. Second, concerning the efficacy, GEEL narrows down the search space to B^2 via intra- and inter-edge gap encodings, where the size of each gap is bounded by graph bandwidth B [15]. We reduce this parameter via the bandwidth restriction scheme [14]. This prevents the model from learning dependencies among a vast vocabulary of size N^2. This improvement is more pronounced when compared with the existing edge list representations, as described in Figure 1c.

We present an autoregressive graph generative model to generate the proposed GEEL with node positional encoding. In detail, we observe that a simple LSTM [16] combined with the proposed GEEL exhibits $O(M)$ complexity. Furthermore, combined with the node positional encoding that indicates the current node index, our GEEL achieved superior performance across ten general graph benchmarks while maintaining simplicity and scalability.

We further extend GEEL to attributed graphs by designing a new grammar and enforcing it to filter out invalid choices during generation. Specifically, our grammar specifies the position of node- and edge-types to be augmented in the GEEL representation. This approach led to competitive performance for two molecule generation benchmarks.

In summary, our key contributions are as follows:

- We newly introduce GEEL, a simple and scalable graph representation that has a compact representation size of M based on edge lists while reducing the large vocabulary size N^2 of the edge lists to B^2 by applying gap encodings. We additionally reduce the graph bandwidth B by the C-M ordering following Diamant et al. [14].
- We propose to autoregressively generate GEEL by incorporating node positional encoding and combining it with an LSTM of $O(M)$ complexity.
- We extend GEEL to deal with attributed graphs by designing a new grammar that takes the node- and edge-types into account.
- We validate the efficacy and scalability of the proposed GEEL and the resulting generative framework by showing the state-of-the-art performance on twelve graph benchmarks.

2 Related works

Adjacency matrix-based graph representation. The adjacency matrix is the most prevalent graph representation, capturing straightforward pairwise relationships between nodes [5, 17, 18, 13, 19, 20, 21]. For instance, You et al. [13] proposed autoregressive generative models, Luo et al. and Shi et al. [21, 20] presented normalizing flow models, and Jo et al. [17] applied score-based models for graph generation. However, these methods suffer from the large representation size associated with generating the *full* adjacency matrix, which is impractical for large-scale graphs.

To solve this problem, several works have introduced scalable graph generative models [22, 23, 14]. Specifically, Liao et al. [22] proposed a block-wise generation that enabled efficiency-quality trade-off. Dai et al. [23] proposed to avoid consideration of every entry in the adjacency matrix, leveraging on the sparsity of graphs. Finally, Diamant et al. [14] proposed to constrain the bandwidth via C-M ordering, bypassing the generation of out-of-bandwidth elements, which reduces the representation complexity to NB.

Tree-based graph representation. Researchers have developed tree-based representations by employing tree search algorithms [8, 24]. Specifically, Segler et al. [8] employed SMILES, a sequential representation for molecules, constructed from the DFS traversal of molecular graphs with omitted cycles. Complementing this, Ahn et al. [24] designed a new representation that exploits the inherent tree-like structure of molecules.

Motif-based graph representation. Researchers have investigated motif-based representations [9, 10, 25], aiming to capture meaningful subgraphs with lower computational costs. In detail, Jin et al. [9, 10] focused on extracting common fragments from datasets. Since these techniques rely on domain-specific knowledge, Guo et al. [25] introduced a domain-agnostic methodology to learn motif-based vocabulary by running reinforcement learning. However, it is still restricted to generating graphs with seen motifs that are included in the training set.

Edge list-based graph representation. A few works have presented edge list-based representations [11, 12]. Employing an edge list as a graph representation reduces the representation size to M, which is smaller than that of the adjacency matrix, N^2. However, these methods suffer from the large vocabulary size N^2, resulting in a large search space and subsequently degrading the generation quality. They also face difficulties in capturing long-term dependencies due to their reliance on depth-first search (DFS) traversal for edge construction. Specifically, DFS traversal fails to closely place edges connected to the same node, so the model must span a broader range of steps to account for edges connected to the same node.

3 Method

In this section, we introduce our new graph representation, gap encoded edge list (GEEL), and the autoregressive generation using GEEL. GEEL has a small representation size M by employing edge lists. In addition, GEEL enjoys a reduced vocabulary size with gap encodings and bandwidth restriction, narrowing down the search space and resulting in the high-quality graph generation.

3.1 Gap encoded edge list representation (GEEL)

First, we present our GEEL representation, which leverages the small representation size of edge lists and the reduced vocabulary size with gap encoding and bandwidth restriction. Consider a graph with N nodes, M edges, and graph bandwidth B [15]. The associated edge list has a representation size of M which is smaller compared to the size of the adjacency matrix N^2. However, it has a large vocabulary size of N^2, consisting of tuples of node indices. To address this, we reduce the vocabulary size into B^2 by replacing the node indices in the original edge list with *gap encodings* as illustrated in Figure 1a. We encode two types of gaps: (1) the inter-edge gap between the source and the target nodes and (2) the intra-edge gap between source nodes in a pair of consecutive edges.

To this end, consider a connected undirected graph $G = (\mathcal{V}, \mathcal{E})$ with N nodes and M edges. We define the *ordering* as an invertible mapping $\pi : \mathcal{V} \to \{1, \ldots, N\}$ from a vertex into its rank for a particular order of nodes. Then we define the *edge list* τ_{EL} as a sequence of pairs of integers:

$$\tau_{\text{EL}} = (s_1, t_1), (s_2, t_2), \ldots, (s_M, t_M),$$

where $s_m, t_m \in \{1, \ldots, N\}$ are the m-th source and target node indices that satisfy $(\pi^{-1}(s_m), \pi^{-1}(t_m)) \in \mathcal{E}$, respectively. Without loss of generality, we assume that $s_m < t_m$ and the edge list is sorted with respect to the ordering, i.e., if $m < \ell$, then $s_m < s_\ell$ or $s_m = s_\ell, t_m < t_\ell$. For example, $(1,2), (1,3), (2,3), (3,5)$ is a sorted edge list while $(1,2), (2,3), (3,5), (1,3)$ is not.

Consequently, we define our GEEL τ_{GEEL} as a sequence of gap encoding pairs as follows:

$$\tau_{\text{GEEL}} = (a_1, b_1), (a_2, b_2), \ldots, (a_M, b_M),$$

where a_m and b_m are the inter- and intra-edge gap encodings, respectively. To be specific, the inter-edge gap encoding indicates the difference between consecutive source indices as follows:

$$a_m = s_m - s_{m-1}, \qquad m = 1, \ldots, M, \qquad s_0 = 0.$$

Furthermore, the intra-edge gap encoding b_m indicates the difference between the associated source and target node indices as follows:

$$b_m = t_m - s_m, \qquad m = 1, \ldots, M.$$

Then one can recover the original edge list τ_{EL} from GEEL τ_{GEEL} as follows:

$$s_m = \sum_{\ell=1}^{m} a_\ell, \qquad t_m = b_m + \sum_{\ell=1}^{m} a_\ell.$$

Note that the gap encodings are always positive and GEEL can be generalized to directed graphs by allowing negative intra-edge gap encodings.

Reduction of the vocabulary size. n training a generative model for edge lists and GEEL, the vocabulary size of (s_m, t_m) and (a_m, b_m) determines the complexity of the model. Here, we show that the vocabulary size of our GEEL is B^2 for the graph bandwidth B, which is smaller than the vocabulary size N^2 of the original edge list representation. Many real-world graphs, such as molecules and community graphs, exhibit low bandwidths as shown in Appendix C and by Diamant et al. [14].

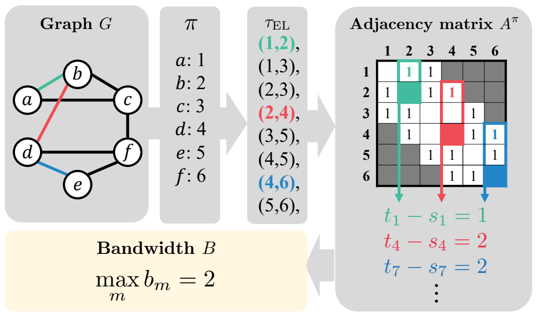

Figure 2: Bandwidth of an adjacency matrix.

The vocabulary size of our GEEL representation is bounded by $\max_m a_m \cdot \max_m b_m$. On one hand, the maximum intra-edge gap encoding coincides with the definition of the graph bandwidth, i.e., the maximum difference between a pair of adjacent nodes, denoted as $\max_m b_m = B$ (Figure 2 illustrates the definition). On the other hand, we can obtain the following upper bound for the inter-edge encoding:

$$\max_m a_m = \max_m (s_m - s_{m-1}) \leq \max_m \left(\max_{\ell < m} t_\ell - s_{m-1} \right) \leq \max_m \max_{\ell < m} (t_\ell - s_\ell) \leq B,$$

where the first inequality is based on deriving $s_m \leq \max_{\ell < m} t_\ell$ from the graph connectivity constraint: each source node index s_m must appear as a target node index in prior for the graph to be connected, i.e., $s_m = t_\ell$ for some $\ell < m$. Consequently, the vocabulary size of our GEEL representation is upper-bounded by $\max_m a_m \cdot \max_m b_m \leq B^2$.

Given that the vocabulary size of GEEL is bounded by B^2, small bandwidth benefits graph generation by reducing the computational cost and the search space. We follow Diamant et al. [14] to restrict the bandwidth via the Cuthill-McKee (C-M) node ordering [26]. We also provide an ablation study with various node orderings in Section 4.3.

3.2 Autoregressive generation of GEEL and node positional encoding

Autoregressive generation. We first describe our method for the autoregressive generation of GEEL. To this end, we propose to maximize the evidence lower bound of the log-likelihood with respect to the latent ordering. To be specific, following prior works on autoregressive graph generative models [13, 22, 23], we maximize the following lower bound:

$$\log p(G) \geq \mathbb{E}_{q(\pi|G)}[\log p(G, \pi)] + C,$$

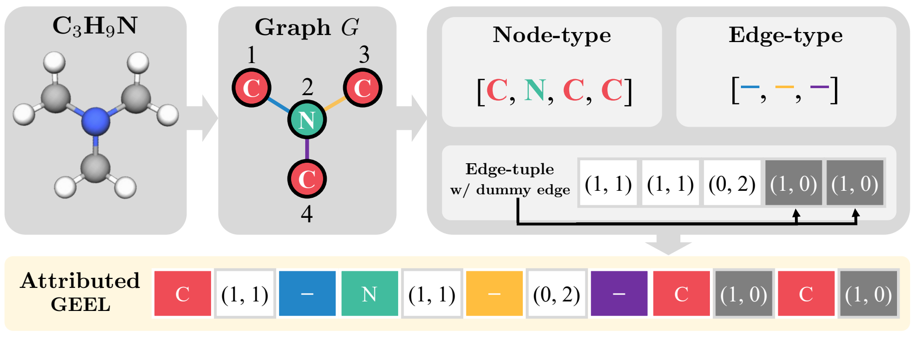

Figure 3: **An example of attributed GEEL.** The colored parts of the attributed GEEL denote the node features (i.e., C and N) and edge features (i.e., single bond -). The shaded parts denote the self-loops added to the original GEEL, where self-loops are added to the nodes that are not connected to the nodes with larger node indices (i.e., nodes with indices 3 and 4).

where C is a constant and $q(\pi|G)$ is a variational posterior of the ordering given the graph G. Under this framework, our choice of choosing the C-M ordering for each graph corresponds to a choice of the variational distribution $q(\pi|G)$. Fixing a particular ordering for each graph yields the maximum log-likelihood objective for $\log p(G,\pi) = \log p(\tau_{\text{GEEL}})$.

We generate GEEL using an autoregressive model formulated as follows:

$$p(\tau_{\text{GEEL}}) = p(a_1, b_1) \prod_{m=2}^{M} p(a_m, b_m | \{a_\ell\}_{\ell=1}^{m-1}, \{b_\ell\}_{\ell=1}^{m-1}).$$

Notably, we treat each tuple (a_m, b_m) as one token and generate a token at each step. Similar to text generative models, we also introduce the begin-of-sequence (BOS) and the end-of-sequence (EOS) tokens to indicate the start and end of the sequence generation process, respectively [27].

Finally, it is noteworthy that we train a long short-term memory (LSTM) model [16] to minimize the proposed objective. Adopting LSTM as our backbone ensures an $O(M)$ complexity for our generative model, due to the linear complexity of the LSTM. The model architecture can be freely changed to more powerful architectures such as Transformers [28], as demonstrated in Section 4.3.

Source node positional encoding. While the gap encoding allows a significant reduction in vocabulary size, it also complicates the inherent semantics since each source node index is represented by the cumulative summation over the intra-edge gap encodings. Instead of burdening the generative model to learn the cumulative summation, we directly supplement the token embeddings with the node positional encoding of the source node index, i.e., $\sum_{\ell=1}^{m} a_\ell$ at the $(m+1)$-th step as:

$$\phi\big((a_m, b_m)\big) = \phi_{\text{tuple}}\big((a_m, b_m)\big) + \phi_{\text{PE}}\Big(\sum_{\ell=1}^{m} a_\ell\Big),$$

where ϕ is the final embedding, ϕ_{tuple} is the token embedding, and ϕ_{PE} is the positional encoding.

3.3 GEEL for attributed graphs

In this section, we elaborate on the extension of GEEL to attributed graphs. To this end, we augment the GEEL representation with node- and edge-types. Our attributed GEEL follows a specific grammar that filters out invalid choices of tokens.

Grammar of attributed GEEL. For the generation of attributed graphs with node- and edge-types, we not only generate the edge-tuples (a_k, b_k) as in Section 3.1 but also generate node- and edge-types according to the following rules. We provide an illustrative example of attribute GEEL in Figure 3.

- Before describing edge-tuples starting with a new source node, add the paired node-type.
- After adding an edge-tuple, add the paired edge-type.

One can observe that our rules are intuitive: for each source node, we first describe the node-type and then generate the associated edge-tuple and types. For nodes that are not associated with any

Table 1: **General graph generation performance.** The baseline results are from prior works [17, 29, 30, 23, 14] or obtained by running the open-source codes. Note that OOM indicates Out-Of-Memory and N.A. for BwR indicates that the generated samples are all invalid. For each metric, the numbers that are superior or comparable to the MMD of the training graphs are highlighted in **bold**. The comparability is determined by whether the MMD falls within one standard deviation.

	Planar			Lobster			Enzymes			SBM		
	$\lvert V\rvert = 64$			$10 \leq \lvert V\rvert \leq 100$			$10 \leq \lvert V\rvert \leq 125$			$31 \leq \lvert V\rvert \leq 187$		
Method	Deg.	Clus.	Orb.	Deg.	Clus.	Orb.	Deg.	Clus.	Orb.	Deg.	Clus.	Orb.
Training	0.001	0.002	0.000	0.005	0.000	0.007	0.006	0.018	0.007	0.016	0.002	0.047
GraphVAE	-	-	-	-	-	-	1.369	0.629	0.191	-	-	-
GraphRNN	0.005	0.278	1.254	**0.000**	**0.000**	**0.000**	0.017	0.062	0.046	**0.006**	0.058	0.079
GRAN	**0.001**	0.043	**0.001**	0.038	**0.000**	**0.001**	0.023	0.031	0.169	**0.011**	0.055	**0.054**
EDP-GNN	-	-	-	-	-	-	0.023	0.268	0.082	-	-	-
GraphGen	1.762	1.423	1.640	0.548	0.040	0.247	0.146	0.079	0.054	1.230	1.752	0.597
GraphGen-Redux	1.105	1.809	0.517	1.189	1.859	0.885	0.456	0.035	0.251	-	-	-
GraphAF	-	-	-	-	-	-	1.669	1.283	0.266	-	-	-
GraphDF	-	-	-	-	-	-	1.503	1.283	0.266	-	-	-
BiGG	0.002	0.004	**0.000**	**0.000**	**0.000**	**0.000**	0.010	**0.018**	0.011	0.029	**0.003**	**0.036**
GDSS	0.250	0.393	0.587	0.117	0.002	0.149	0.026	0.061	**0.009**	0.496	0.456	0.717
DiGress	**0.000**	**0.002**	0.008	**0.021**	**0.000**	**0.004**	0.011	0.039	0.010	**0.006**	0.051	**0.058**
GDSM	-	-	-	-	-	-	0.013	0.088	0.010	-	-	-
GraphARM	-	-	-	-	-	-	0.029	0.054	0.015	-	-	-
BwR + GraphRNN	0.609	0.542	0.097	0.316	**0.000**	0.247	0.021	0.095	0.025	N.A.	N.A.	N.A.
BwR + Graphite	0.971	0.562	0.636	0.076	1.075	0.060	0.213	0.270	0.056	1.305	1.341	1.056
BwR + EDP-GNN	1.127	1.032	0.066	0.237	0.062	0.166	0.253	0.118	0.168	0.657	1.679	0.275
GEEL (ours)	**0.001**	0.010	**0.001**	**0.002**	**0.000**	**0.001**	**0.005**	**0.018**	**0.006**	0.025	**0.003**	**0.026**

(a) Small graphs ($|V|_{\max} \leq 187$)

	Ego			Grid			Proteins			3D point cloud		
	$50 \leq \lvert V\rvert \leq 399$			$100 \leq \lvert V\rvert \leq 400$			$13 \leq \lvert V\rvert \leq 1575$			$8 \leq \lvert V\rvert \leq 5037$		
Method	Deg.	Clus.	Orb.	Deg.	Clus.	Orb.	Deg.	Clus.	Orb.	Deg.	Clus.	Orb.
Training	0.010	0.003	0.016	0.000	0.000	0.000	0.002	0.003	0.002	0.004	0.090	0.015
GraphVAE	-	-	-	1.619	**0.000**	0.919	-	-	-		OOM	
GraphRNN	0.117	0.615	0.043	0.011	0.000	0.021	0.011	0.140	0.880		OOM	
GRAN	0.026	0.342	0.254	0.001	0.004	0.002	0.002	0.049	0.130	0.018	0.510	0.210
EDP-GNN	-	-	-	0.455	0.238	0.328	-	-	-	-	-	-
GraphGen	0.578	1.199	0.776	1.550	0.017	0.860	1.392	1.743	0.866		OOM	
GraphGen-Redux	1.088	0.702	0.155	-	-	-	-	-	-	-	-	-
SPECTRE	-	-	-	-	-	-	0.013	0.047	0.029	-	-	-
BiGG	**0.010**	0.017	**0.012**	**0.000**	**0.000**	0.001	**0.001**	0.026	0.023	**0.003**	0.210	**0.007**
GDSS	0.393	0.873	0.209	0.111	0.005	0.070	0.703	1.444	0.410		OOM	
DiGress	0.063	0.031	0.024	0.016	**0.000**	0.004		OOM			OOM	
GDSM	-	-	-	0.002	**0.000**	**0.000**	-	-	-	-	-	-
BwR + GraphRNN	N.A.	N.A.	N.A.	0.385	1.187	0.083	0.092	0.229	0.489	1.820	1.295	0.869
BwR + Graphite	0.229	0.123	0.054	0.483	1.142	0.083	0.239	0.245	0.492		OOM	
BwR + EDP-GNN		OOM		0.574	0.983	0.602	0.184	0.208	0.738		OOM	
SwinGNN	-	-	-	**0.000**	**0.000**	**0.000**	**0.002**	0.016	**0.003**	-	-	-
GEEL (ours)	0.053	0.017	**0.016**	**0.000**	**0.000**	**0.000**	**0.003**	**0.005**	**0.003**	**0.002**	**0.081**	**0.020**

(b) Large graphs ($399 \leq |V|_{\max} \leq 5037$)

edge-tuple as a source node, we add a "dummy" edge-tuple with the node as its source. As a result, our representation size for attributed graphs is at most $2M + N$ and the vocabulary size is $2B$.

Autoregressive generation with grammar constraints. To enforce the attribute grammar, we introduce an algorithm to filter out invalid choices of tokens.

- The first token is always the node-type token.
- The node-type tokens are always followed by edge-tuple tokens.
- The edge-tuple tokens are always followed by edge-type tokens.
- The edge-type tokens are always followed by node-type tokens or edge-tuple tokens.

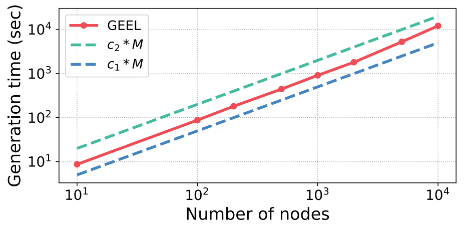

Figure 4: **Infer. time on various graph sizes.**

Table 2: **Inference time (sec) to generate one graph**.

Method	Type	Enzymes	Planar	Grid
GRAN	Auto. Reg.	0.24	0.66	1.39
BiGG	Auto. Reg.	2.70	0.61	3.58
GDSS	Diffusion	15.21	15.25	30.89
DiGress	Diffusion	8.82	12.09	32.29
GEEL (ours)	Auto. Reg.	**0.12**	**0.25**	**1.11**

These rules prevent the generation process from generating invalid GEEL such as the list that consists of only node-types or the list that has an edge-tuple without a following edge-type token. This procedure is done by computing the probability only over valid choices.

4 Experiment

4.1 General graph generation

Evaluation protocol. We adopt maximum mean discrepancy (MMD) as our evaluation metric to compare three graph property distributions between test and generated graphs: degree, clustering coefficient, and 4-node-orbit counts. **Results that are either superior to or comparable with the MMD of training graphs** are highlighted in bold in Table 1. The comparability of MMD values is determined by examining whether the MMD falls within a range of one standard deviation. Notably, our work stands out as a baseline for graph generative models, given its comprehensive evaluation across ten diverse graph datasets and its state-of-the-art performance. Further details regarding our experimental setup are in Appendix A.

We validate the general graph generation performance of our GEEL on eight general graph datasets with varying sizes: $10 \leq |V| \leq 5037$. Four small-sized graphs are: (1) **Planar**, 200 synthetic planar graphs, (2) **Lobster**, 100 random Lobster graphs [31], (3) **Enzymes** [32], 587 protein tertiary structure graphs, and (4) **SBM**, 200 stochastic block model graphs. Four large-sized graphs are: (5) **Ego**, 757 large Citeseer network dataset [33], (6) **Grid**, 100 synthetic 2D grid graphs, (7) **Proteins**, 918 protein graphs, and (8) **3D point cloud**, 41 3D point cloud graphs of household objects. Additional experimental results on two smaller datasets (**Ego-small** and **Community-small**) are provided in Appendix E.

We compare our GEEL with sixteen deep graph generative models. They can be categorized into two according to the type of representation they use. On one hand, fourteen adjacency matrix-based methods are: GraphVAE [5], GraphRNN [13], GNF [34], GRAN [22], EDP-GNN [19], GraphAF [20], GraphDF [21], SPECTRE [30], BiGG [23], GDSS [17], DiGress [18], GDSM [35], GraphARM [29], and BwR [14]. On the other hand, two edge list-based methods are GraphGen [11] and GraphGen-Redux [12]. We provide a detailed implementation description in Appendix B.

Generation quality. We provide experimental results in Table 1. We observe that the proposed GEEL consistently shows superior or competitive results across all the datasets. This verifies the ability of our model to effectively capture the topological information of both large and small graphs. The visualization of generated samples can be found in Appendix D. It is worth noting that the generation performance on small graphs has reached a saturation point, yielding results that are either superior or comparable to training graphs.

Scalability analysis. Next, we empirically validate the time complexity of our model. We first verify if the actual inference time aligns well with the theoretical $O(M)$ curve. To this end, we generated Grid graphs with varying numbers of nodes: [10, 100, 200, 500, 1k, 2k, 5k, 10k]. The results shown in Figure 4 indicate an alignment between the actual inference time and the ideal curve.

Then we conduct further experiments to compare the inference time of our model with that of other baselines. Note that we used the same computational resource for all models and other experimental details are in Appendix B. The results presented in Table 2 represent the time required to generate a single sample. Notably, our model shows a shorter inference time owing to the compactness of

Table 4: **Molecular graph generation performance of the QM9 and ZINC datasets.** The baseline results are from prior works [17, 24]. The best results of molecule-specific generative models and domain-agnostic generative models are both highlighted in **bold**.

Method	QM9						ZINC250k					
	Val. (%) (↑)	NSPDK (↓)	FCD (↓)	Scaf. (↑)	SNN (↑)	Frag. (↑)	Val. (%) (↑)	NSPDK (↓)	FCD (↓)	Scaf. (↑)	SNN (↑)	Frag. (↑)
Molecule-specific generative models												
CharRNN	99.57	**0.0003**	**0.087**	0.9313	0.5162	0.9887	96.95	**0.0003**	0.474	0.4024	0.3965	**0.9988**
CG-VAE	**100.0**	-	1.852	0.6628	0.3940	0.9484	**100.0**	-	11.335	0.2411	0.2656	0.8118
MoFlow	91.36	0.0169	4.467	0.1447	0.3152	0.6991	63.11	0.0455	20.931	0.0133	0.2352	0.7508
STGG	**100.0**	-	0.585	0.9416	**0.9998**	**0.9984**	**100.0**	-	**0.278**	**0.7192**	**0.4664**	0.9932
Domain-agnostic graph generative models												
EDP-GNN	47.52	0.0046	2.680	0.3270	0.5265	0.8313	63.11	0.0485	16.737	0.0000	0.0815	0.0000
GraphAF	74.43	0.0207	5.625	0.3046	0.4040	0.8319	68.47	0.0442	v16.023	0.0672	0.2422	0.5348
GraphDF	93.88	0.0636	10.928	0.0978	0.2948	0.4370	90.61	0.1770	33.546	0.0000	0.1722	0.2049
GDSS	95.72	0.0033	2.900	0.6983	0.3951	0.9224	97.01	0.0195	14.656	0.0467	0.2789	0.8138
DiGress	98.19	0.0003	0.095	0.9353	0.5263	0.0023	94.99	0.0021	3.482	0.4163	0.3457	0.9679
DruM	99.69	**0.0002**	0.108	**0.9449**	**0.5272**	0.9867	98.65	**0.0015**	2.257	0.5299	0.3650	0.9777
GraphARM	90.25	0.0020	1.220	-	-	-	88.23	0.0550	16.260	-	-	-
GEEL (ours)	**100.0**	**0.0002**	**0.089**	0.9386	0.5161	**0.9891**	**99.31**	0.0068	**0.401**	**0.5565**	**0.4473**	**0.992**

our representation, GEEL, even compared to other scalable graph generative models [22, 23]. This evidence underscores the scalability advantages of our GEEL.

In addition, we provide the reduced representation and vocabulary sizes in Table 3. Note that the vocabulary size of the original edge list and the representation size of the adjacency matrix are both N^2. We can observe that GEEL is significantly efficient in terms of both representation and vocabulary sizes.

Table 3: **Vocabulary and representation sizes.** The vocabulary size is B^2 and the representation size is M where B is bandwidth, N is the number of nodes, and M is the number of edges.

Dataset	Vocab. size	Rep. size	N^2
Planar	676	181	4096
Lobster	2401	99	9604
Enzymes	361	149	15625
SBM	12321	1129	34969
Ego	58081	1071	$> 10^6$
Grid	361	684	467856
Proteins	62500	1575	$> 10^6$
3D point cloud	111556	10886	$> 10^7$

4.2 Molecular graph generation

To show that GEEL is capable of representing attributed graphs, we extend our evaluation to molecular graphs that have node- and edge-types. This ensures a comprehensive assessment of the ability of GEEL to generate attributed graphs in chemistry and bioinformatics.

Experimental setup. We use two molecular datasets: QM9 [36] and ZINC250k [37]. Following the previous work [17], we evaluate 10,000 generated molecules using six metrics: (a) the ratio of valid molecules without correction (**Val.**), (b) neighborhood subgraph pairwise distance kernel (**NSPDK**), (c) Frechet ChemNet Distance (**FCD**) [38], (d) scaffold similarity (**Scaf.**), (e) similarity to the nearest neighbor (**SNN**), and (f) fragment similarity (**Frag.**). We use the same split with Jo et al. [17] for a fair comparison. Note that in contrast to other general graph generation methods, our approach uniquely facilitates the direct representation of ions by employing them as a node type. We provide details in Appendix A.

Baselines. We compare GEEL with seven general deep graph generative models: EDP-GNN [19], GraphAF [20], GraphDF [21], GDSS [17], DiGress [18], DruM [39], and GraphARM [29]. In addition, for further comparison, we also compare GEEL with four molecule-specific generative models: CharRNN [8], CG-VAE [10], MoFlow [40], and STGG [24]. We provide a detailed implementation description in Appendix B.

Results. The experimental results are reported in Table 4. We observe that our GEEL shows superior results to domain-agnostic graph generative models and competitive results with molecule-specific generative models. In particular, for the QM9 dataset, we observe that our GEEL shows superior results on FCD and Scaffold scores even compared to the molecule-specific models. We also provide the visualization of generated molecules in Appendix D.

Table 5: **Average MMD results for different model architectures.**

Backbone	Planar	Enzymes	Grid
LSTM	0.002	0.009	0.000
Transformer	0.003	0.008	0.000

Table 6: **Average MMD for different representations**. We adopted LSTM as a model architecture and OOM denotes out-of-memory error.

Representation	Repr.	Vocab.	Com.-small	Grid	Point
Flattened adj.	N^2	2	0.029	OOM	OOM
Edge list	M	N^2	0.010	0.000	OOM
Edge list + intra gap	M	NB	0.013	0.000	OOM
GEEL (ours)	M	B^2	0.016	0.000	0.044

4.3 Ablation studies

Different model architectures. Here, we discuss the results of generating GEEL with Transformers [28]. We evaluate four datasets: Planar, Lobster, Enzymes, and Grid, employing three MMD metrics for assessment. As presented in Table 5, LSTM shows competitive results to Transformers. Notably, LSTM achieves this performance with significantly reduced computational cost, having a linear complexity of $O(n)$, in contrast to the quadratic complexity $O(n^2)$ of Transformers, where n represents the sequence length.

Different representations. We discuss the results of generating graphs with various representations here. We compare our GEEL with three alternative representations: flattened adjacency matrix, the edge list, and the edge list with node-wise distance using LSTM. The last one is an edge list wherein the target node of each edge is substituted by its intra-edge gap. Note that the edge lists are sorted in the same way we sort the edge list, as explained in Section 3.1. The comparative results are in Table 6. We can observe that GEEL effectively reduces the vocabulary size compared to other edge list-based representations. This enables the generation of large-scale graphs, such as 3D point clouds, without encountering memory constraints.

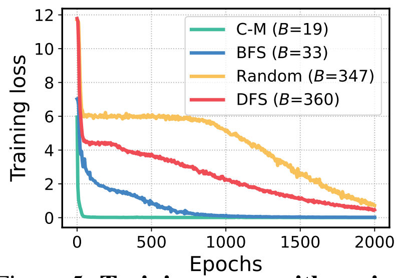

Figure 5: **Training curve with various node orderings.**

Different node orderings. We here assess the effect of node ordering on graph generation. We compare our C-M ordering to BFS, DFS, and random ordering using the Grid dataset. As illustrated in Figure 5, the C-M ordering outperforms other orderings with faster convergence of training loss and small bandwidth. Notably, the BFS also shows competitive loss convergence with C-M as it mitigates the burden of long-term dependency. Specifically, both C-M and BFS orderings position edges related to the same node more closely than other baselines. These results highlight the effectiveness of C-M ordering on bandwidth reduction and generating high-quality graphs.

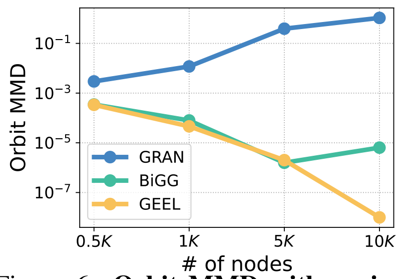

Figure 6: **Orbit MMD with various graph sizes.**

Quality with various graph sizes. We also evaluate the generated graph quality with respect to the graph size. Following a prior work [23], we conduct experiments on grid data with {0.5k, 1k, 5k, 10k} nodes and reported orbit MMD. The results are in Figure 6 and we can see GEEL preserves high quality on large-scale graphs with up to 10k nodes.

5 Conclusion

In this work, we introduce GEEL, an edge list-based graph representation that is both simple and scalable. By combining GEEL with an LSTM, our graph generative model achieves an $O(M)$ complexity, showing a significant enhancement in generation quality and scalability over prior graph generative models. An interesting direction for future work is to present a new graph generation benchmark as the performance for small graphs is already saturated.

References

[1] Aditya Grover, Aaron Zweig, and Stefano Ermon. Graphite: Iterative generative modeling of graphs. In *International conference on machine learning*, pages 2434–2444. PMLR, 2019. 1

[2] Yujia Li, Oriol Vinyals, Chris Dyer, Razvan Pascanu, and Peter Battaglia. Learning deep generative models of graphs. *arXiv preprint arXiv:1803.03324*, 2018. 1

[3] Łukasz Maziarka, Agnieszka Pocha, Jan Kaczmarczyk, Krzysztof Rataj, Tomasz Danel, and Michał Warchoł. Mol-cyclegan: a generative model for molecular optimization. *Journal of Cheminformatics*, 12(1):1–18, 2020. 1

[4] Jonathan Ho, Ajay Jain, and Pieter Abbeel. Denoising diffusion probabilistic models. *Advances in neural information processing systems*, 33:6840–6851, 2020. 1

[5] Martin Simonovsky and Nikos Komodakis. Graphvae: Towards generation of small graphs using variational autoencoders. In *Artificial Neural Networks and Machine Learning–ICANN 2018: 27th International Conference on Artificial Neural Networks, Rhodes, Greece, October 4-7, 2018, Proceedings, Part I 27*, pages 412–422. Springer, 2018. 1, 3, 7, 14

[6] Kaushalya Madhawa, Katushiko Ishiguro, Kosuke Nakago, and Motoki Abe. Graphnvp: An invertible flow model for generating molecular graphs. *arXiv preprint arXiv:1905.11600*, 2019. 1

[7] Meng Liu, Keqiang Yan, Bora Oztekin, and Shuiwang Ji. Graphebm: Molecular graph generation with energy-based models. *arXiv preprint arXiv:2102.00546*, 2021. 1

[8] Marwin HS Segler, Thierry Kogej, Christian Tyrchan, and Mark P Waller. Generating focused molecule libraries for drug discovery with recurrent neural networks. *ACS central science*, 4(1):120–131, 2018. 1, 3, 8, 14

[9] Wengong Jin, Regina Barzilay, and Tommi Jaakkola. Junction tree variational autoencoder for molecular graph generation. In *International conference on machine learning*, pages 2323–2332. PMLR, 2018. 1, 3

[10] Wengong Jin, Regina Barzilay, and Tommi Jaakkola. Hierarchical generation of molecular graphs using structural motifs. In *International conference on machine learning*, pages 4839–4848. PMLR, 2020. 1, 3, 8, 14

[11] Nikhil Goyal, Harsh Vardhan Jain, and Sayan Ranu. Graphgen: a scalable approach to domain-agnostic labeled graph generation. In *Proceedings of The Web Conference 2020*, pages 1253–1263, 2020. 1, 3, 7, 14

[12] Davide Bacciu and Marco Podda. Graphgen-redux: A fast and lightweight recurrent model for labeled graph generation. In *2021 International Joint Conference on Neural Networks (IJCNN)*, pages 1–8. IEEE, 2021. 1, 3, 7

[13] Jiaxuan You, Rex Ying, Xiang Ren, William Hamilton, and Jure Leskovec. Graphrnn: Generating realistic graphs with deep auto-regressive models. In *International conference on machine learning*, pages 5708–5717. PMLR, 2018. 1, 3, 4, 7, 13, 14

[14] Nathaniel Lee Diamant, Alex M Tseng, Kangway V Chuang, Tommaso Biancalani, and Gabriele Scalia. Improving graph generation by restricting graph bandwidth. In *International Conference on Machine Learning*, pages 7939–7959. PMLR, 2023. 2, 3, 4, 6, 7

[15] Phyllis Z Chinn, Jarmila Chvátalová, Alexander K Dewdney, and Norman E Gibbs. The bandwidth problem for graphs and matrices—a survey. *Journal of Graph Theory*, 6(3):223–254, 1982. 2, 3

[16] Sepp Hochreiter and Jürgen Schmidhuber. Long short-term memory. *Neural computation*, 9(8):1735–1780, 1997. 2, 5, 14

[17] Jaehyeong Jo, Seul Lee, and Sung Ju Hwang. Score-based generative modeling of graphs via the system of stochastic differential equations. In *International Conference on Machine Learning*, pages 10362–10383. PMLR, 2022. 3, 6, 7, 8, 13, 14, 21

[18] Clement Vignac, Igor Krawczuk, Antoine Siraudin, Bohan Wang, Volkan Cevher, and Pascal Frossard. Digress: Discrete denoising diffusion for graph generation. *arXiv preprint arXiv:2209.14734*, 2022. 3, 7, 8, 13, 14

[19] Chenhao Niu, Yang Song, Jiaming Song, Shengjia Zhao, Aditya Grover, and Stefano Ermon. Permutation invariant graph generation via score-based generative modeling. In *International Conference on Artificial Intelligence and Statistics*, pages 4474–4484. PMLR, 2020. 3, 7, 8, 14

[20] Chence Shi, Minkai Xu, Zhaocheng Zhu, Weinan Zhang, Ming Zhang, and Jian Tang. Graphaf: a flow-based autoregressive model for molecular graph generation. *arXiv preprint arXiv:2001.09382*, 2020. 3, 7, 8, 14

[21] Youzhi Luo, Keqiang Yan, and Shuiwang Ji. Graphdf: A discrete flow model for molecular graph generation. In *International Conference on Machine Learning*, pages 7192–7203. PMLR, 2021. 3, 7, 8, 14

[22] Renjie Liao, Yujia Li, Yang Song, Shenlong Wang, Will Hamilton, David K Duvenaud, Raquel Urtasun, and Richard Zemel. Efficient graph generation with graph recurrent attention networks. *Advances in neural information processing systems*, 32, 2019. 3, 4, 7, 8, 14

[23] Hanjun Dai, Azade Nazi, Yujia Li, Bo Dai, and Dale Schuurmans. Scalable deep generative modeling for sparse graphs. In *International conference on machine learning*, pages 2302–2312. PMLR, 2020. 3, 4, 6, 7, 8, 9, 13, 14

[24] Sungsoo Ahn, Binghong Chen, Tianzhe Wang, and Le Song. Spanning tree-based graph generation for molecules. In *International Conference on Learning Representations*, 2022. 3, 8, 14

[25] Minghao Guo, Veronika Thost, Beichen Li, Payel Das, Jie Chen, and Wojciech Matusik. Data-efficient graph grammar learning for molecular generation. *arXiv preprint arXiv:2203.08031*, 2022. 3

[26] Elizabeth Cuthill and James McKee. Reducing the bandwidth of sparse symmetric matrices. In *Proceedings of the 1969 24th national conference*, pages 157–172, 1969. 4

[27] Michael Collins. Head-driven statistical models for natural language parsing. *Computational linguistics*, 29(4):589–637, 2003. 5

[28] Ashish Vaswani, Noam Shazeer, Niki Parmar, Jakob Uszkoreit, Llion Jones, Aidan N Gomez, Łukasz Kaiser, and Illia Polosukhin. Attention is all you need. *Advances in neural information processing systems*, 30, 2017. 5, 9

[29] Lingkai Kong, Jiaming Cui, Haotian Sun, Yuchen Zhuang, B. Aditya Prakash, and Chao Zhang. Autoregressive diffusion model for graph generation, 2023. 6, 7, 8, 14

[30] Karolis Martinkus, Andreas Loukas, Nathanaël Perraudin, and Roger Wattenhofer. Spectre: Spectral conditioning helps to overcome the expressivity limits of one-shot graph generators. In *International Conference on Machine Learning*, pages 15159–15179. PMLR, 2022. 6, 7, 14

[31] Elizabeth Senger. Polyominoes: Puzzles, patterns, problems, and packings. *The Mathematics Teacher*, 90(1):72, 1997. 7

[32] Ida Schomburg, Antje Chang, Christian Ebeling, Marion Gremse, Christian Heldt, Gregor Huhn, and Dietmar Schomburg. Brenda, the enzyme database: updates and major new developments. *Nucleic acids research*, 32(suppl_1):D431–D433, 2004. 7

[33] Prithviraj Sen, Galileo Namata, Mustafa Bilgic, Lise Getoor, Brian Galligher, and Tina Eliassi-Rad. Collective classification in network data. *AI magazine*, 29(3):93–93, 2008. 7, 21

[34] Jenny Liu, Aviral Kumar, Jimmy Ba, Jamie Kiros, and Kevin Swersky. Graph normalizing flows. *Advances in Neural Information Processing Systems*, 32, 2019. 7, 14

[35] Tianze Luo, Zhanfeng Mo, and Sinno Jialin Pan. Fast graph generative model via spectral diffusion. *arXiv preprint arXiv:2211.08892*, 2022. 7, 14

[36] Raghunathan Ramakrishnan, Pavlo O Dral, Matthias Rupp, and O Anatole Von Lilienfeld. Quantum chemistry structures and properties of 134 kilo molecules. *Scientific data*, 1(1):1–7, 2014. 8

[37] John J Irwin, Teague Sterling, Michael M Mysinger, Erin S Bolstad, and Ryan G Coleman. Zinc: a free tool to discover chemistry for biology. *Journal of chemical information and modeling*, 52(7):1757–1768, 2012. 8

[38] Kristina Preuer, Philipp Renz, Thomas Unterthiner, Sepp Hochreiter, and Gunter Klambauer. Fréchet chemnet distance: a metric for generative models for molecules in drug discovery. *Journal of chemical information and modeling*, 58(9):1736–1741, 2018. 8

[39] Jaehyeong Jo, Dongki Kim, and Sung Ju Hwang. Graph generation with destination-driven diffusion mixture. *arXiv preprint arXiv:2302.03596*, 2023. 8, 14

[40] Chengxi Zang and Fei Wang. Moflow: an invertible flow model for generating molecular graphs. In *Proceedings of the 26th ACM SIGKDD International Conference on Knowledge Discovery & Data Mining*, pages 617–626, 2020. 8, 14

[41] Adam Paszke, Sam Gross, Francisco Massa, Adam Lerer, James Bradbury, Gregory Chanan, Trevor Killeen, Zeming Lin, Natalia Gimelshein, Luca Antiga, et al. Pytorch: An imperative style, high-performance deep learning library. *Advances in neural information processing systems*, 32, 2019. 14

A Experimental Details

In this section, we provide the details of the experiments.

A.1 General graph generation

Table 7: **Hyperparameters of GEEL in general graph generation.**

	Planar	Lobster	Enzymes	SBM	Ego	Grid	Proteins	3D point cloud
Learning rate	0.001	0.0001	0.0005	0.0001	0.0001	0.001	0.0001	0.0012
Batch size	128	64	128	8	8	64	8	4

Table 8: **Default hyperparameters of GEEL.**

Input dropout rate	Dim. of token embedding	Num. of layers
0.1	512	3

We used the same split with GDSS [17] for Enzymes and Grid datasets, with DiGress [18] for Planar and SBM datasets, with BiGG [23] for Lobster, Proteins, and 3D point cloud datasets, and with GraphRNN [13] for ego dataset. We perform the hyperparameter search to choose the best learning rate in {0.0001, 0.0005, 0.001, and 0.0012}. We select the model with the best MMD with the lowest average of three graph statistics: degree, clustering coefficient, and 4-orbit count. In addition, we report the means of 5 different runs. We provide the best learning rates in Table 7 and other default hyperparameters that we have not tuned in Table 8.

A.2 Molecular graph generation

We used the same split with GDSS [17] for a fair evaluation. Following general graph generation, we perform the hyperparameter search to choose the best learning rate in {0.0001, 0.001} and select the model with the best FCD score. The best learning rates are 0.001 for both QM9 and ZINC datasets and other default hyperparameters are in Table 8 which is the same as the general graph generation.

For ion tokenization, we used 13 node tokens for QM9: [C-], [CH-], [C], [F], [N+], [N-], [NH+], [NH2+], [NH3+], [NH], [N], [O-], [O]. In addition, we used 29 tokens for ZINC: [Br], [CH-], [CH2-], [CH], [C], [Cl], [F], [I], [N+], [N-], [NH+], [NH-], [NH2+], [NH3+], [NH], [N], [O+], [O-], [OH+], [O], [P+], [PH+], [PH2], [PH], [P], [S+], [S-], [SH+], [S].

B Implementation Details

B.1 Computing resources

We used Pytorch [41] to implement GEEL and trained the LSTM [16] models on GeForce RTX 3090 GPU. Note that we used A100-40GB for the 3D point cloud dataset. In addition, due to the CUDA compatibility issue of BiGG [23], we used GeForce GTX 1080 Ti GPU and 40 CPU cores for inference time evaluation in Figure 1c.

B.2 Details for baseline implementation

Table 9: **Reproduced dataset for each baselines.**

	Planar	Lobster	Enzymes	SBM	Ego	Grid	Proteins	3D point cloud
GRAN	-	-	O	-	O	-	-	-
GraphGen	O	O	O	O	O	O	O	O
BiGG	O	-	O	O	O	-	-	-
GDSS	O	O	-	O	O	-	O	O
DiGress	-	O	O	-	O	O	O	O

General graph generation. The baseline results from prior works are as follows. We reproduced GRAN [22], GraphGen [11], DiGress [18], GDSS [17] and BiGG [23] for the datasets that are not reported in the original paper using their open-source codes. The reproduced datasets are explained in Table 9. The other results for GraphVAE [5], GNF [34], EDP-GNN [19], GraphAF [20], GraphDF [21], and GDSS [17] are obtained from GDSS, while the results for GRAN [22], GraphRNN [13], and BiGG [23] are from BiGG and SPECTRE [30]. Finally, the remaining results for SPECTRE and GDSM [35] are derived from their respective paper. We used original hyperparameters when the original work provided them.

Molecular graph generation. The baseline results from prior works are as follows. The results for five domain-agnostic graph generative models: EDP-GNN [19], GraphAF [20], GraphDF [21], GDSS [17], DruM [39] are from DruM, and the GraphARM [29] result is extracted from the corresponding paper. Moreover, we reproduced DiGress [18] using their open-source codes.

In addition, for molecule generative models, the result of MoFlow [40] is from DruM, the results of CG-VAE [10] and STGG [24] is from STGG. Furthermore, we reproduced CharRNN [8].

C Graph statistics of datasets

C.1 General graphs

Table 10: **Statstics of general datasets.**

Dataset	# of graphs	# of nodes	Max. B	Max. # of edges
Planar	200	$\|V\| = 64$	26	181
Lobster	100	$10 \leq \|V\| \leq 100$	49	99
Enzymes	587	$10 \leq \|V\| \leq 125$	19	149
SBM	200	$31 \leq \|V\| \leq 187$	111	1129
Ego	757	$50 \leq \|V\| \leq 399$	241	1071
Grid	100	$100 \leq \|V\| \leq 400$	19	684
Proteins	918	$13 \leq \|V\| \leq 1575$	125	1575
3D point cloud	41	$8 \leq \|V\| \leq 5037$	167	10886

Table 11: **Standard deviation of MMD in training dataset.**

Planar			Lobster			Enzymes			SBM		
Deg.	Clus.	Orb.	Deg.	Clus.	Orb.	Deg.	Clus.	Orb.	Deg.	Clus.	Orb.
0.000	0.001	0.000	0.003	0.000	0.006	0.001	0.003	0.002	0.008	0.002	0.017

(a) Small graphs ($|V|_{\max} \leq 187$)

Ego			Grid			Proteins			3D point cloud		
Deg.	Clus.	Orb.	Deg.	Clus.	Orb.	Deg.	Clus.	Orb.	Deg.	Clus.	Orb.
0.005	0.001	0.004	0.000	0.000	0.000	0.001	0.002	0.001	0.04	0.062	0.017

(b) Large graphs ($|V|_{\max} \leq 187$)

The statistics of general graphs are summarized in Table 10. It is notable that the bandwidths are relatively low compared to the number of nodes for real-world graphs, which enables the reduction of the vocabulary size of GEEL. In addition, we provide the standard deviations of MMD of training graphs that we used as a criterion to verify comparability in Table 11.

C.2 Molecular graphs

Table 12: **Statstics of molecular datasets: QM9 and ZINC250k**.

Dataset	# of graphs	# of nodes	Max. B	Max. # of edges	# of node types	# of edge types
QM9	133,885	$1 \leq \|V\| \leq 9$	5	13	13	4
ZINC250k	249,455	$6 \leq \|V\| \leq 38$	10	45	29	4

The statistics of molecular graphs are summarized in Table 12. Note that the # of node types indicate the number of ionized node type tokens as explained in Appendix A.

D Generated samples

D.1 General graph generation

Planar

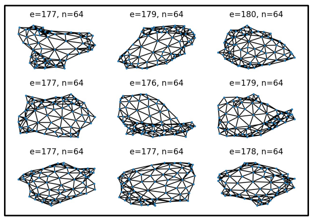

(a) Train

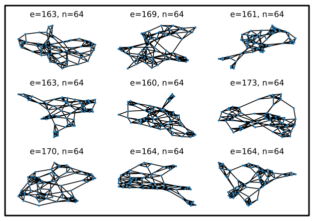

(b) GDSS

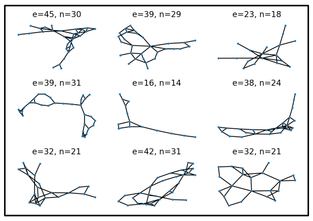

(c) GraphGen

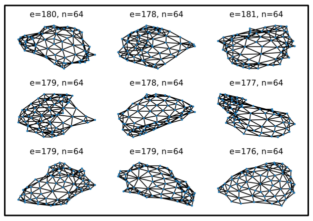

(d) BiGG

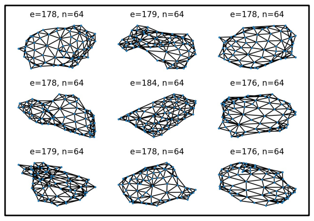

(e) DiGress

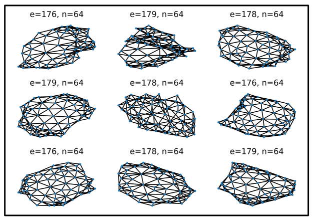

(f) GEEL (ours)

Figure 7: **Visualization of the graphs from the Planar dataset and the generated graphs.**

Lobster

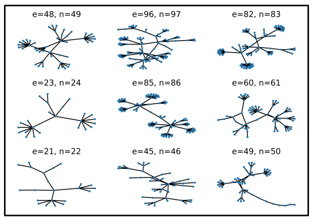

(a) Train

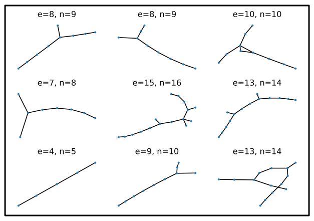

(b) GraphGen

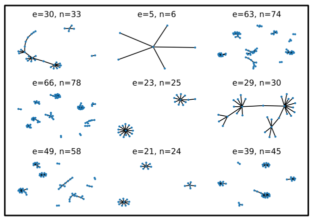

(c) GDSS

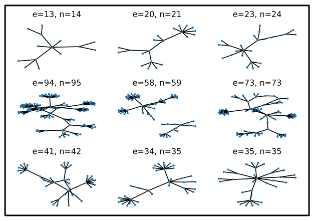

(d) DiGress

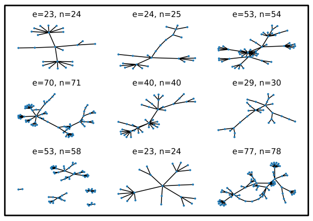

(e) GEEL (ours)

Figure 8: **Visualization of the graphs from the Lobster dataset and the generated graphs.**

Enzymes

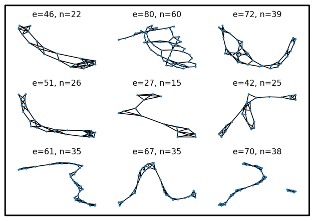

(a) Train

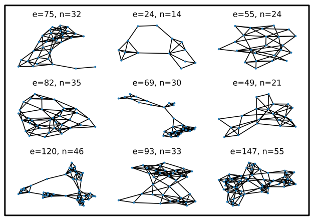

(b) GRAN

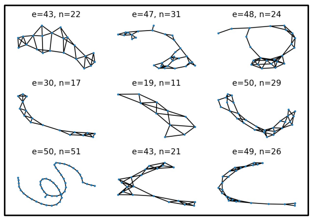

(c) GraphGen

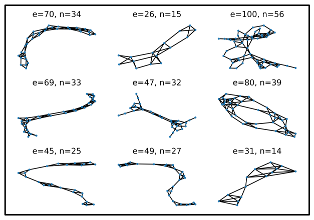

(d) BiGG

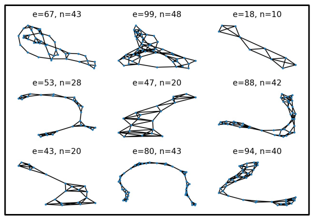

(e) DiGress

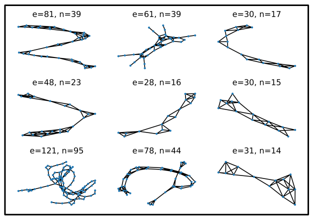

(e) GEEL (ours)

Figure 9: **Visualization of the graphs from the Enzymes dataset and the generated graphs.**

SBM

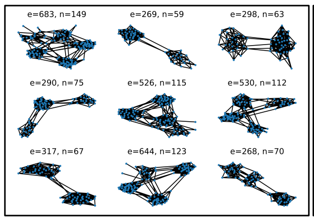

(a) Train

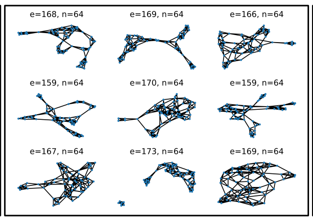

(b) GDSS

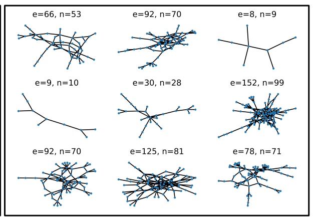

(c) GraphGen

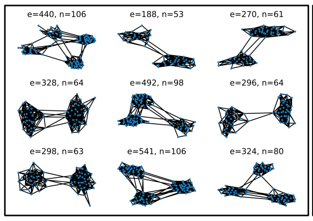

(d) BiGG

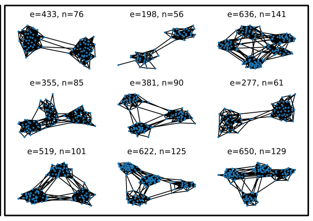

(e) GEEL (ours)

Figure 10: **Visualization of the graphs from the SBM dataset and the generated graphs.**

Ego

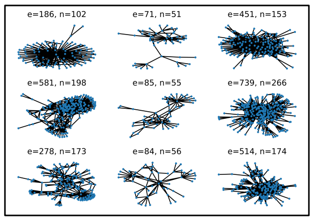

(a) Train

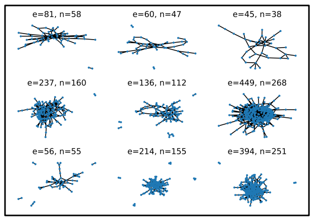

(b) GRAN

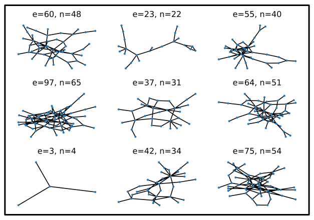

(c) GraphGen

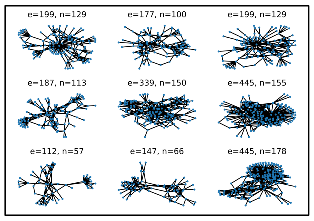

(d) BiGG

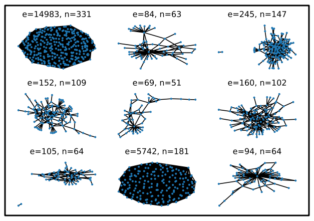

(e) GDSS

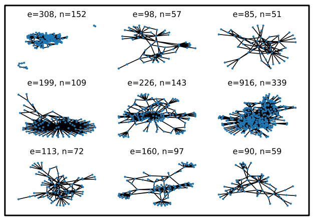

(e) GEEL (ours)

Figure 11: **Visualization of the graphs from the Ego dataset and the generated graphs.**

Grid

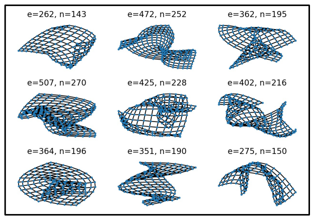

(a) Train

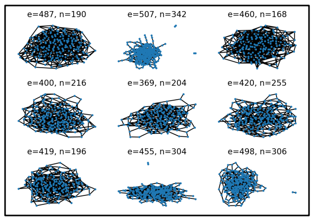

(b) GDSS

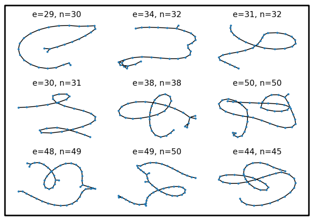

(c) GraphGen

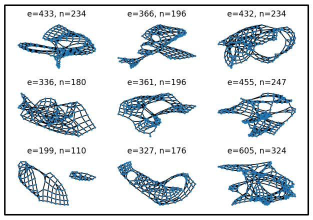

(d) DiGress

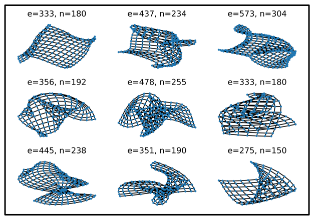

(e) GEEL (ours)

Figure 12: **Visualization of the graphs from the Grid dataset and the generated graphs.**

Proteins

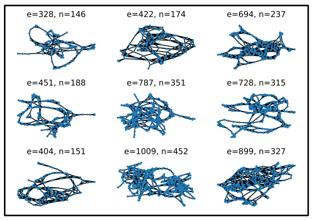

(a) Train

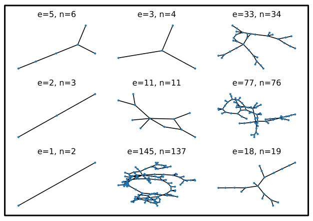

(b) GraphGen

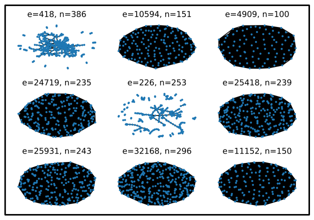

(c) GDSS

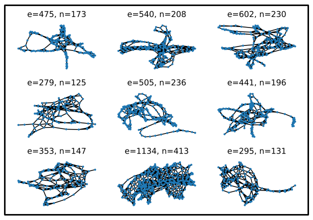

(d) GEEL (ours)

Figure 13: **Visualization of the graphs from the Proteins dataset and the generated graphs.**

We present visualizations of graphs from the training dataset and generated samples from GRAN, GraphGen, BiGG, GDSS, DiGress, and GEEL in Figure 7, Figure 8, Figure 9, Figure 10, Figure 11, Figure 12, and Figure 13. Note that we only provide the visualization that we have reproduced, which is detailed in Appendix B. We additionally give the number of nodes and edges of each graph, where n denotes the number of nodes and e denotes the number of edges.

D.2 Molecular graph genereation

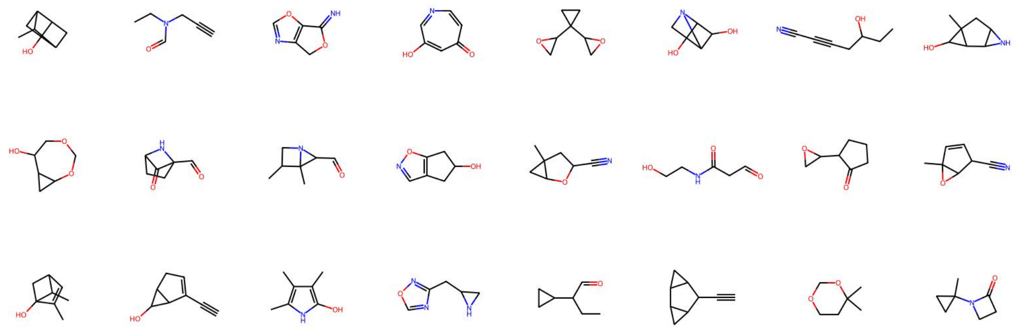

Figure 14: **Visualization of the molecules generated from the QM9 dataset.**

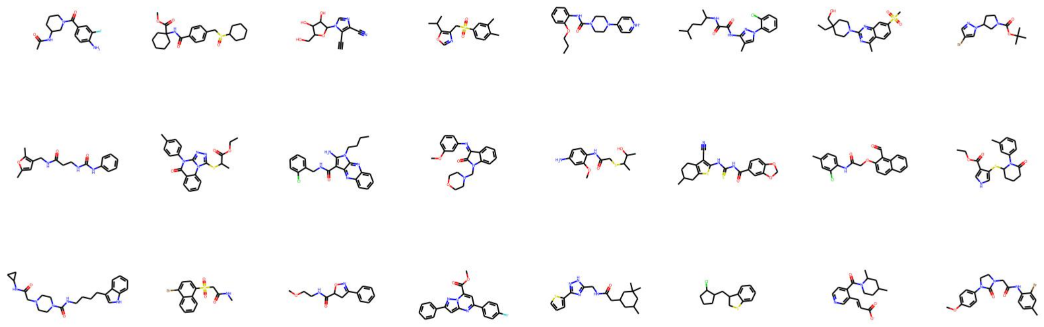

Figure 15: **Visualization of the molecules generated from the ZINC250k dataset.**

We provide visualizations of generated molecules using GEEL in Figure 14 and Figure 15.

E Additional Experimental Results

	Ego-small			Community-small		
	$4 \leq \lvert V \rvert \leq 18$			$12 \leq \lvert V \rvert \leq 20$		
Method	Deg.	Clus.	Orb.	Deg.	Clus.	Orb.
Training	0.025	0.035	0.012	0.020	0.044	0.003
GraphVAE	0.130	0.170	0.050	0.350	0.980	0.540
GraphRNN	0.090	0.220	**0.003**	0.080	0.120	0.040
GRAN	**0.009**	**0.038**	**0.009**	**0.005**	0.142	0.090
GNF	**0.030**	0.100	**0.001**	0.200	0.200	0.110
EDP-GNN	0.052	0.093	**0.007**	0.053	0.144	0.026
GraphGen	0.085	0.102	0.425	0.075	0.065	0.014
GraphAF	**0.030**	0.110	**0.001**	0.180	0.200	0.020
GraphDF	0.040	0.130	**0.010**	0.060	0.120	0.030
BiGG	**0.013**	**0.030**	**0.005**	**0.004**	**0.005**	**0.000**
GDSS	**0.021**	**0.024**	**0.007**	0.045	0.086	0.007
DiGress	**0.021**	**0.026**	**0.024**	**0.012**	**0.025**	**0.002**
GDSM	-	-	-	**0.011**	**0.015**	**0.001**
GraphARM	**0.019**	**0.017**	**0.010**	0.034	0.082	**0.004**
GEEL (ours)	**0.020**	**0.035**	**0.012**	**0.020**	**0.022**	0.006

Table 13: General graph generation on small graphs ($\lvert V \rvert_{\max} \leq 20$)

We provide general graph generation results for smaller graph datasets: Ego-small and Community-small. The **Ego-small** dataset consists of 300 small ego graphs from larger Citeseer network [33] and **Community-small** dataset consists of 100 randomly generated community graphs. We used the same split with GDSS [17] and the results are reported in Table 13.